Available online at www.sciencedirect.com
ScienceDirect
Biochimica et Biophysica Acta 1778 (2008) 166–174
Biochimica et Biophysica Acta
BBA
www.elsevier.com/locate/bbamem

Liquid–liquid immiscibility in model membranes activates secretory phospholipase A_2

Kerstin Wagner [a,*], Bernard Desbat [b], Gerald Brezesinski [a]

[a] *Max Planck Institute of Colloids and Interfaces, 14424 Potsdam, Germany*
[b] *Chimie et Biochimie des Membranes et Nanosystèmes, UMR 5248 CNRS - Université Bordeaux 1, 33607 Pessac, France*

Received 21 June 2007; received in revised form 17 September 2007; accepted 19 September 2007
Available online 16 October 2007

Abstract

Secretory phospholipase A_2 ($sPLA_2$) hydrolyzes phosphatidylcholines (PC) within lipid bilayers to produce lyso-PC and a fatty acid, which can act as signaling molecule in biological membranes. The activity of $sPLA_2$ depends on the membrane structure. Bilayer defects, curvature, and gel–fluid micro-heterogeneity are known to activate $sPLA_2$. Here, we investigate if liquid–liquid immiscibility within model membranes is sufficient for $sPLA_2$ activation. The onset of the hydrolytic activity of cobra-venom $sPLA_2$ towards mixed monolayers of dimyristoyl-PC (DMPC)/cholesterol 2:1 (mol/mol) has been determined using infrared reflection–absorption spectroscopy (IRRAS) and polarization-modulated (PM-) IRRAS. The lag phase of $sPLA_2$ activity increases exponentially with rising surface pressures starting at 12 mN/m. This indicates that enzyme activation is hampered at higher surface pressures. Below 12 mN/m, no lag phase is observed, and $sPLA_2$ is efficiently activated. The surface pressure that is critical for $sPLA_2$ activation correlates with the critical miscibility pressure according to the phase diagram of DMPC and cholesterol. Thus, coexisting, liquid-phase domains provide sufficient boundaries to activate $sPLA_2$. Moreover, liquid–liquid immiscibility is an activating mechanism for $sPLA_2$ that also applies to biological membranes under physiological conditions because the corresponding bilayer structure is associated with that of membrane rafts.

Keywords: Dimyristoylphosphatidylcholine (DMPC); Cholesterol; Monolayer structure; Phase separation; Infrared reflection–absorption spectroscopy (IRRAS); Lipolytic enzyme activation

1. Introduction

Phospholipase A_2 (PLA_2) is a lipid-modifying enzyme that hydrolyzes the carboxylic ester linkage in the *sn*-2 position of phospholipids within membranes. The catalytic activity is stereospecific to the naturally abundant L-enantiomer of phospholipids [1]. The reaction products, a lyso-phospholipid and a fatty acid, remain within the lipid bilayer provided that they exhibit a sufficient length of the acyl chains. In biological membranes, products of the PLA_2 activity like arachidonic acid serve as signaling molecules in various, physiological processes [2–5].

The PLA_2 superfamily comprises a broad range of enzymes that catalyze the described reaction. They are currently classified into 15 different groups [6]. In general, two types of PLA_2 can be distinguished: the extracellular and the typically intracellular enzymes [7]. The secretory PLA_2s ($sPLA_2$) are characterized by an active-site histidine and an absolute requirement of Ca^{2+} for catalytic activity. These enzymes carry out a major role in venoms and digestive fluids; they are also involved in the regulation of inflammation and immune response [2–5]. In contrast, most cytosolic PLA_2s ($cPLA_2$) utilize a catalytic serine for hydrolytic cleavage. Ca^{2+} is excluded from the active site, but some enzymes require the cation for membrane translocation [7]. The activity of $cPLA_2$s is associated with intracellular trafficking events by altering membrane structure, shape, and function [8]. Vice versa, it is further assumed that PLA_2 action depends on membrane topology. Thus, an increasing interest in examining the influence of membrane structure on the activity of lipid-modifying enzymes has developed during the last decades.

Most biophysical investigations in this field have used $sPLA_2$s from group I or II, which include isoforms of the enzyme

* Corresponding author. Tel.: +49 331 5679212; fax: +49 331 5679202.
E-mail address: wagner@mpikg.mpg.de (K. Wagner).

0005-2736/$ - see front matter © 2007 Elsevier B.V. All rights reserved.
doi:10.1016/j.bbamem.2007.09.015

from snake-venom, mammalian pancreatic, and human synovial fluids. Extensive work has been carried out utilizing vesicular substrates [9,10]. Thus, phosphatidylcholines (PC) in the gel–fluid phase transition region were found to modulate PLA_2 activity [11]. Fluorescence spectroscopy and pH-stat titration applied to large unilamellar vesicles (LUV) revealed that the lateral rearrangement of lipids causes an enzyme activation [12]. In fact, the lag time of PLA_2 decreases due to dynamic bilayer heterogeneities that occur on a nanometer scale in the phase transition region of PC [13,14]. The described lag phase of PLA_2 commences after the addition of enzyme to the substrate and indicates a period of little hydrolysis before PLA_2 activity bursts (i.e. lag–burst behavior).

Similar to the activation process, a dynamic inhibition of PLA_2 has been proposed [9]. This originates from transient and local reaction-product aggregations owing to a limited, lateral diffusion of lipids within the membrane. Furthermore, the accumulation of lipid products can eventually generate a lateral gel–fluid phase separation. The accompanying formation of domains increases the internal interface and creates alterations in the bilayer thickness [15]. This event is one more activating mechanism for PLA_2 as it was also shown for other multi-component LUVs [16]. Hence, PLA_2 activation through gel–fluid heterogeneity in membranes can either be due to non-equilibrium density fluctuations during phase transition or to the presence of thermodynamically stable domains in phase separations [10].

This notion of PLA_2 activity at lipid bilayers is consistent with the results of lipid monolayer studies that observed PLA_2 action *in situ* by epifluorescence microscopy. It was proven that the liquid-expanded/condensed phase transition region in dipalmitoyl-PC (DPPC) films constitutes the preferred binding environment of PLA_2 [17,18]. The enzymatic hydrolysis is initiated at the phase boundary and directed towards the interior of condensed lipid domains. The hydrolytic process can be quantified by (polarization-modulated) infrared reflection–absorption spectroscopy, i.e. (PM-) IRRAS, since the technique has been shown to be applicable to examine PLA_2 activity [19,20]. The maximum turnover of DPPC monolayers is achieved at the phase transition pressure [21]. Thus, it was confirmed that PLA_2 is sensitive to the defect lines and domain boundaries within the lipid substrate.

Beyond micro-heterogeneity, further concepts of PLA_2 activation including membrane defects and curvature [22–24] as well as lipid protrusion [25,26] have evolved. Although membrane curvature and the protrusion of lipids are well perceived in the highly dynamic system of biological membranes, gel–fluid phase separations are not presumed. Hence, it remains obscure how PLA_2 can be activated through micro-heterogeneity under physiological conditions.

Here, we attempt to address this question using mixed monolayers as model membranes that exhibit a liquid–liquid immiscibility. This phenomenon was first described for monolayer mixtures of dimyristoyl-PC (DMPC) and cholesterol (chol) [27,28]. By means of epifluorescence microscopy, two coexisting liquid phases can be observed: one rich in DMPC, the other rich in cholesterol. When the monolayer is compressed, the two-phase coexistence disappears. Respective transition pressures π_t have been determined for different molar mixing ratios to establish pressure-composition phase diagrams [29]. An extract of the phase diagram of DMPC/chol monolayers is shown in Fig. 1. For a 2:1 (mol/mol) mixture of DMPC/chol, the different liquid phases persist up to ~11 mN/m. Consequently, PLA_2 should be activated below this π_t. Above ~11 mN/m, a homogeneous liquid phase appears, which is expected to hamper PLA_2 activation. To verify the effect of liquid–liquid immiscibility on PLA_2 activity, we exploit the correlation of PLA_2 activation with the termination of the lag phase [13]. In the present research paper, the lag time Δt of cobra-venom PLA_2 action towards DMPC/chol (2:1, mol/mol) monolayers is determined by different IRRAS techniques.

2. Materials and methods

2.1. Materials

L-1,2-Dimyristoyl-*sn*-glycero-3-phosphocholine (DMPC), 1-myristoyl-*sn*-glycero-3-phosphocholine (lyso-MPC), and cholesterol (all from Sigma-Aldrich, Steinheim, Germany) were used as received and dissolved in chloroform (JTBaker, Deventer, Holland) to give 1 mM stock solutions. These solutions were utilized to prepare mixtures of DMPC/chol with a molar mixing ratio of 2:1. PLA_2 from *Naja mossambica mossambica* (cobra) venom, i.e. group IA, was purchased from Sigma-Aldrich and used without further purification. Aliquots of the enzyme dissolved in buffer were prepared and stored at −20 °C until their application. The aqueous buffer solution consisted of 10 mM Tris (Sigma-Aldrich), 150 mM NaCl (Merck, Darmstadt, Germany), and 100 μM $CaCl_2$ (Sigma-Aldrich) and was adjusted to pH 8.9 with 1 N HCl (Merck). Water was purified with a Millipore system to give a resistivity of 18.2 MΩ cm.

The used buffer provides optimal conditions for PLA_2, although buffers containing 5 mM $CaCl_2$ were used during previous work on PLA_2 of different origins [19,20,30]. A 100-μM $CaCl_2$ concentration is sufficient for PLA_2 activity as tested with DPPC monolayers by IRRAS (data not shown). This concentration is in the range of optimum conditions for PLA_2 from other snake venoms [15,31].

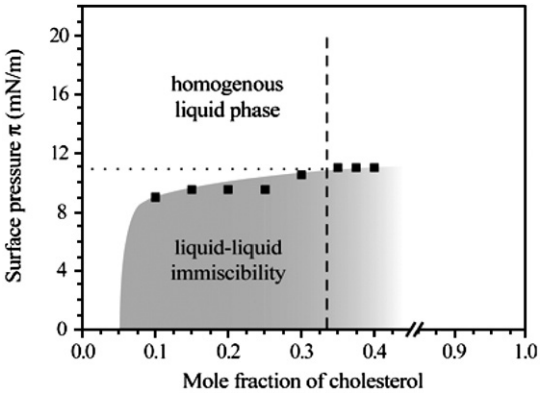

Fig. 1. Phase diagram of DMPC/chol monolayers adapted from Okonogi and McConnell [29]. Data points (■) depict transition pressures π_t as measured by epifluorescence microscopy for different monolayers spread on water at 24.5 °C. Two coexisting liquid phases are observed below π_t (corresponding section shaded in grey); a single liquid phase is detected above π_t (white area of the phase diagram). The current paper investigates DMPC/chol (2:1, mol/mol) monolayers at different surface pressures (set along the dashed line) below and above the appropriate π_t (dotted line).

2.2. Langmuir film balance

The surface pressure/area (π/A) isotherms were recorded on film balances from R&K (Potsdam, Germany) and NIMA Technology (Coventry, England) during IRRAS and PM-IRRAS measurements, respectively. Both setups were equipped with a Wilhelmy-type pressure-measuring system using a filter paper as plate. After spreading the phospholipid-containing solution on the aqueous-buffered subphase, chloroform was allowed to evaporate for 10 min. The monolayer was subsequently compressed at a velocity of ~4 Å^2/molecule/min while the π/A isotherm was continuously recorded. After the desired surface pressure was reached, a first (PM-) IRRA control spectrum was measured. Subsequently, the enzyme solution (1 unit) was injected into the subphase and carefully stirred underneath the monolayer. The hydrolytic process was detected by (PM-) IRRA spectroscopy. Two automatically moving barriers kept the surface pressure constant during the reaction process. The temperature T was maintained at 20 °C during all IRRAS experiments. PM-IRRAS measurements were conducted at room temperature.

2.3. IRRA spectroscopy

Spectra were acquired with an IFS 66 FT-IR spectrometer from Bruker (Ettlingen, Germany) equipped with an external reflectance unit containing a Langmuir trough setup (R&K). The infrared beam is directed through the external port of the spectrometer and is subsequently reflected by three mirrors in a rigid mount before being focused on the water surface. The desired angle of incidence is obtained by a computer-driven rotation of the mount holding the mirrors. A KRS-5 wire grid polarizer is placed into the optical path directly before the beam hits the water surface. The reflected light is collected at the same angle as the angle of incidence. The light then follows an equivalent mirror path and is directed onto a narrow band mercury–cadmium–telluride (MCT) detector, which is cooled by liquid nitrogen. The entire experimental setup is enclosed to reduce relative humidity fluctuations. A shuttling procedure is used to compensate residual water vapor rotation–vibration bands [32]. For this purpose, the home-built trough is divided into two compartments that are connected to ensure the same surface height on both sides. One compartment is monolayer-covered (sample); the other one is monolayer-free (reference). By applying the shuttle mechanism, the interferograms of sample and reference can be alternately collected. In all measurements, *s*-polarized radiation was used at an angle of incidence of 40°.

A total of 200 scans were acquired with a scanner velocity of 20 kHz at a resolution of 8 cm^{-1}. The scans were co-added, apodized with the Blackman–Harris 3-term function, and fast Fourier-transformed with one level of zero-filling to produce spectral data encoded at 4 cm^{-1} intervals. IRRA spectra are presented as absorbance vs. wavenumber. Absorbance, also reflectance–absorbance, is obtained from $-\lg(R/R_0)$, where R is the single-beam reflectance of the sample and R_0 the single-beam reflectance of the reference. The spectra were not baseline-corrected to exclude any manipulation of peak heights.

2.4. PM-IRRA spectroscopy

Spectra were acquired with a Nicolet Nexus 870 spectrometer from Thermo Fisher Scientific (Waltham, MA, USA) equipped with an external reflectance unit containing a Langmuir trough setup (NIMA Technology). The infrared beam is conducted out of the spectrometer and focused onto the water surface. The angle of incidence is 75° to the surface normal. The incident beam line is polarized by a BaF_2 wire grid polarizer and modulated between parallel (*p*) and perpendicular (*s*) polarization by a 37-kHz ZnSe photoelastic modulator (Hinds Instruments, Hillsboro, OR, USA). The reflected light is collected by a BaF_2 lens and focused on a photovoltaic MCT detector (Société Anonyme de Télécommunications (SAT), Poitiers, France). Two-channel processing with a lock-in amplifier (Sirenza Microdevices, Sunnyvale, CA, USA) demodulates the detected signal and provides the differential reflectivity spectrum $\Delta R/R$. The PM-IRRAS signal S equals $\Delta R/R$ given by $S=\Delta R/R=(R_p-R_s)J_2/(R_p+R_s+(R_p-R_s)J_0)$ where R_p and R_s depict the reflectivity for *p*- and *s*-polarized light [33,34]. The difference of each monolayer spectrum S_d and its corresponding subphase spectrum S_0 (recorded in absence of the monolayer) is calculated and normalized according to $\Delta S/S=(S_d-S_0)/S_0$. Thus, the contribution of the liquid water absorption and the dependence on the second-order Bessel function J_2 are eliminated [33,34].

For each spectrum, at least 200 scans were collected with a resolution of 8 cm^{-1}. The scans were co-added, apodized with the Happ–Genzel function, and fast Fourier-transformed with two levels of interpolation to produce spectral data encoded at 1 cm^{-1} intervals. A PM-IRRA spectrum of water vapor is subtracted from the original monolayer spectra to remove residual rotation–vibration bands of the vapor. The resulting PM-IRRA spectra are smoothed and presented as (normalized difference of the) PM-IRRAS signal $\Delta S/S$ vs. wavenumber. The spectra were not baseline-corrected to exclude further manipulation of peak heights.

3. Results

3.1. IRRAS of DMPC and lyso-MPC

During the enzymatic reaction, the lipid substrate PC is hydrolyzed to yield the lipid product lyso-PC and a fatty acid. PC has two carboxylic ester bonds whereas lyso-PC contains only one acyl ester linkage in the *sn*-1 position. Therefore, (PM-) IRRAS spectra of PC and lyso-PC show a significant difference in the band intensity of the carbonyl vibration ν(C═O) [19,20]. In former PM-IRRAS studies, the amount of PC in monolayers mixed with the reaction products was correlated to the ν(C═O) band intensity to compile calibration curves [21,35]. Subsequently, the hydrolysis of DPPC and distearoyl-PC monolayers by PLA_2 was quantified at different surface pressures. In contrast to those investigations, the present work uses DMPC as PLA_2 substrate. The IRRA spectra of DMPC and lyso-MPC monolayers reveal specific characteristics of the ν(C═O) band that have not been considered in this context before (Fig. 2). Hence, the following paragraphs describe the effect of carbonyl hydration on the ν(C═O) band and explain why it is impossible to create calibration curves for our system.

Fig. 2A shows the spectral fingerprint region of DMPC and lyso-MPC. The negative ν(C═O) band of DMPC is positioned at 1733 cm^{-1} and exhibits an asymmetric shape. The band is located next to the bending vibration of liquid water at 1645 cm^{-1} and superposes the water vapor rotation–vibrations centered at 1595 cm^{-1} [36]. For different measurements, the water vapor rotation–vibration bands slightly vary in intensity because humidity fluctuations cannot be completely avoided in our experimental setup. Therefore, all spectra are aligned with respect to the positive band at 1770 cm^{-1}, which is right next to the negative ν(C═O) vibration, to exclude a modification of the ν(C═O) band intensity due to humidity variations.

The asymmetry of the ν(C═O) band of DMPC is an effect of hydration, i.e. the hydrogen bonding of water molecules to the carbonyl groups [37,38]. In Fig. 2B, the fitting of two overlapped Gaussian peaks resolve two components constituting the ν(C═O) vibration. They are located at 1737 and 1725 cm^{-1}, respectively. The higher wavenumber corresponds to the non-hydrated C═O group, the lower one to the hydrogen-bonded C═O. Because both forms have different absorption coefficients, the fraction of hydrated C═O groups is not directly deducible from the intensity ratio of the two bands [37]. Previous studies of specifically ^{13}C═O labeled DMPC molecules forming bilayers in D_2O provide contradicting results. Transmission

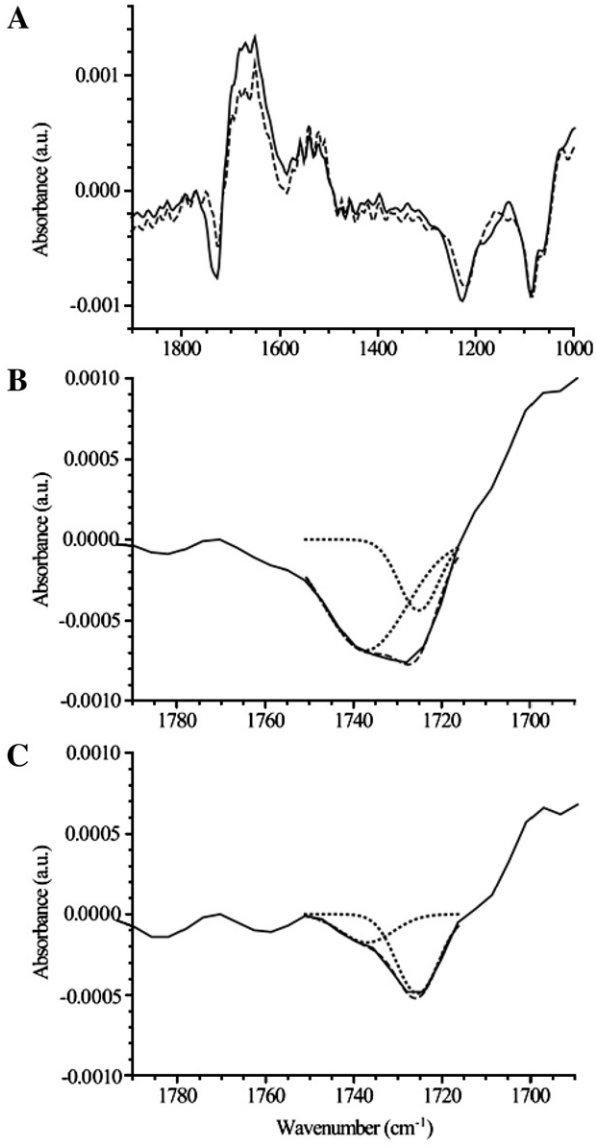

Fig. 2. IRRA spectra of monolayers of pure DMPC and lyso-MPC on the buffered subphase at 10 mN/m and 20 °C. (A) Experimental spectra of DMPC (solid line) and lyso-MPC (dashed line) are aligned at 1770 cm^{-1}. (B, C) Fitted Gaussian curves of two overlapped peaks (dotted lines) constituting the ν(C═O) band of DMPC (B) and lyso-MPC (C). Solid lines represent sections of (A); dashed lines are the sum of the fitted individual peaks.

FT-IR experiments show that the *sn*-2 C═O group is more hydrated than the *sn*-1 C═O [37]. In contrast, time-resolved two-color FT-IR and molecular dynamics simulations reveal that the *sn*-1 C═O group has a higher propensity to form hydrogen bonds with water than the *sn*-2 C═O [39]. In either case, the *sn*-1 as well as the *sn*-2 carbonyl occur in both hydration states. Hence, it is unfeasible to assign either ν(C═O) peak to either of the C═O groups.

Fig. 2C depicts the two components of the ν(C═O) band of lyso-MPC. They are located at the same wavenumbers as the hydrated and non-hydrated ν(C═O) of DMPC, but their intensity ratio is completely different. The peak at 1725 cm^{-1} is much more pronounced [37]. So clearly, lyso-MPC is more hydrated than DMPC. This conclusion is corroborated by the position of the asymmetric phosphate stretching vibration $\nu_{as}(PO_2^-)$ characterizing another part of the lipid headgroup (Fig. 2A). The band appears at 1228 cm^{-1} for DMPC monolayers and at 1222 cm^{-1} for lyso-MPC. The shift to lower wavenumbers confirms the higher hydration state of lyso-MPC [40,41]. As a consequence of the altering degree of hydration of the C═O group in DMPC and lyso-MPC, the ν(C═O) band intensity and the amount of DMPC in a mixed monolayer do not exhibit a linear relationship. Therefore, it is not possible to produce a calibration curve that allows the quantification of the hydrolytic turnover of DMPC in our system.

Furthermore, the reaction products can dissolve in the subphase [42,43]. Their degree of dissolution is supposed to vary at different stages of the hydrolytic process. Thus, the surface concentration of the other lipids is increased in an undefined manner, and a universal calibration curve cannot be established. Nevertheless, a decrease in the ν(C═O) band intensity unambiguously indicates the onset of the hydrolytic reaction provided that the PLA_2 adsorption to the monolayer does not lead to a change in hydration or conformation of the C═O group of DMPC.

3.2. PLA_2 activity probed by IRRAS

At the end of the lag phase of PLA_2, the enzyme is activated and starts to efficiently hydrolyze DMPC. This moment is observable by the beginning decrease of the ν(C═O) band intensity at 1733 cm^{-1}. This fact applies as well to the hydrolysis of mixed monolayers of DMPC and cholesterol. Because cholesterol does not comprise any carbonyl group, the detected ν(C═O) band is exclusive to the lipid moiety of the mixture. Fig. 3 illustrates the examination of the onset of PLA_2 activity at mixed monolayers of DMPC/chol 2:1 (mol/mol) in dependence of the surface pressure.

The spectra of an exemplary experiment conducted at 14 mN/m are shown in Fig. 3A. Before the injection of PLA_2, the spectrum of the DMPC/chol (2:1, mol/mol) monolayer exhibits similar features as seen for pure DMPC. Only the ν(C═O) band reveals a slightly different shape. This is most likely due to the presence of cholesterol, which might influence the hydration state of the C═O group via complex formation with DMPC [28,29]. To follow the enzymatic hydrolysis, IRRA spectra are collected every 5 min after the addition of 1 unit PLA_2 to the subphase. 5 min are the shortest possible time interval for the IRRAS technique operating in the trough shuttling procedure. The first spectrum completed 6 min after enzyme injection does not display any significant changes to the original spectrum. This implies that the adsorption of PLA_2 does not cause a modification of the ν(C═O) band. (Further evidence is introduced later in this section.) Within 11 min after PLA_2 addition, the ν(C═O) band intensity is considerably reduced indicating the onset of DMPC hydrolysis. Thus in this experiment, the lag phase in PLA_2 activity Δt amounts to a minimum of 6 min.

The progression of the enzymatic reaction at 14 mN/m is denoted by a further decrease of the ν(C═O) band intensity (Fig. 3A). This trend halts within ~40 min after the injection of PLA_2 signifying the termination of the DMPC turnover. The

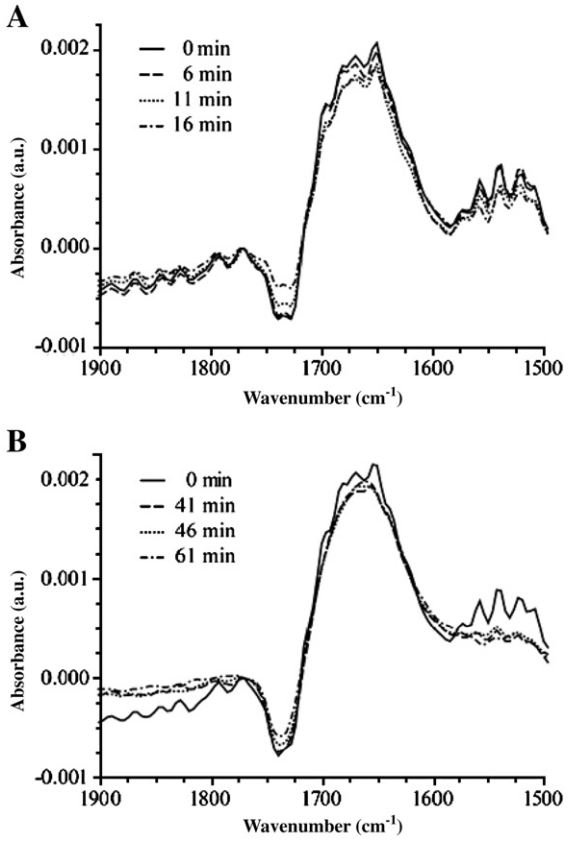

Fig. 3. IRRA spectra of DMPC/chol (2:1, mol/mol) monolayers before and after injection of 1 unit PLA_2 into the buffered subphase. (A) Spectra were acquired at a surface pressure of 14 mN/m before (solid line) and within 6; 11; and 16 min after PLA_2 injection (interrupted lines). (B) Spectra were acquired at 16 mN/m before (solid line) and within 41; 46; and 61 min after PLA_2 injection (interrupted lines). All spectra are aligned at 1770 cm^{-1}.

spectra acquired at an advanced state of the hydrolytic process are expected to be dominated by the characteristic vibrations of the reaction products. However, the ν(C═O) band does not exhibit a more pronounced component at 1725 cm^{-1} as seen for pure lyso-MPC but remains centered at 1733 cm^{-1}. It is possible that the hydration state of the C═O groups in lyso-MPC is also altered in the presence of cholesterol; but it is more likely that lyso-MPC dissolves in the subphase and the final band is due to remaining substrate in the monolayer. Furthermore, additional peaks at ~1540 and 1575 cm^{-1} do not evolve during hydrolysis. The doublet is usually observed in the presence of the second reaction product and depicts the ν_{as} (COO^-) vibration of the fatty acid–calcium complex [20]. The missing peaks confirm that myristic acid is not stable in the monolayer but dissolves in the subphase [42]. Because of this loss of material, the film is continuously compressed in the constant pressure mode of the film balance when hydrolysis occurs (cf. Fig. 5). In summary, the presented spectra display the shortest detectable, i.e., a 6-min lag phase of PLA_2 activity towards DMPC/chol (2:1, mol/mol) monolayers at 14 mN/m.

Fig. 3B depicts the same experiment performed at 16 mN/m. In this example, the spectra collected before and within 41 min after PLA_2 injection exhibit water vapor rotation–vibration bands at different levels of absorbance. This is due to the different time periods of atmosphere equilibration. The longer the time interval between enzyme injection and measurement, the more smooth the IRRA spectra become. The alignment of all spectra at 1770 cm^{-1} obviates the influence of the water vapor absorption on the ν(C═O) band intensity. Hence, the latter does not vary within 41 min after PLA_2 injection. This time period is sufficiently long to allow PLA_2 adsorption to the monolayer. Though the unchanged spectra demonstrate that this event does not modify the ν(C═O) band. Within 46 min after enzyme injection, the ν(C═O) band reveals a first intensity decrease indicating the end of the PLA_2 lag phase ($\Delta t \geq 41$ min). A further reduction of the ν(C═O) band intensity is detected with each subsequent measurement, but the change in absorbance every 5 min is much smaller than at 14 mN/m. This suggests that the hydrolytic reaction is proceeding with a slower rate at the slightly higher surface pressure of 16 mN/m.

The described experiments were repeated at different surface pressures to obtain a more reliable result on the lag time of PLA_2 activity. Mean values of Δt are plotted in Fig. 4. At 12 mN/m, the DMPC/chol (2:1, mol/mol) monolayers are immediately hydrolyzed by 1 unit PLA_2, and a lag phase is not detectable using IRRA spectroscopy. At 14 mN/m, the average period before the onset of the hydrolytic reaction amounts to 7 min. This lag time increases exponentially with rising surface pressure. Higher amounts of enzyme injected into the subphase would presumably reduce Δt, but lag phases shorter than 6 min cannot be resolved by the IRRAS technique. On the other hand, the application of lower enzyme concentrations should increase Δt [43]. Thus, it might be possible to observe a lag phase at 12 mN/m that is not detected on the current conditions. Nonetheless, we did not use smaller amounts of PLA_2 to avoid that enzyme activation is more heavily dependent on the preceding step, i.e. PLA_2 adsorption to the monolayer. In the latter case, the final rate of the activation process would be determined by enzyme diffusion rather than by model membrane structure. Therefore, we strived for another approach to corroborate our

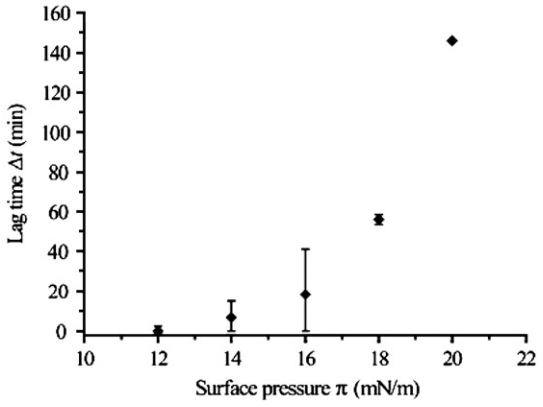

Fig. 4. Dependence of the lag time of PLA_2 activity Δt on the surface pressure π in mixed monolayers of DMPC/chol 2:1 (mol/mol) on a buffered subphase containing 1 unit PLA_2. Data points represent mean values of Δt from n IRRAS experiments conducted at 20 °C. $n \geq 4$ for 14 and 16 mN/m; $n = 2$ for 12 and 18 mN/m; and $n = 1$ for 20 mN/m.

results without changing the optimum range of enzyme concentration applied so far.

It has to be added that PLA_2 exhibits a higher activity towards cholesterol-containing than pure DMPC monolayers, where hydrolysis is not observed within ~39 min after enzyme injection at 16 mN/m (Fig. 5). The lag time Δt of the PLA_2 activity towards pure DMPC monolayers cannot be determined by IRRAS because the solubility of both reaction products leads to a continuous loss of these substances from the film. On account of the lack of reaction products or cholesterol, the proportion of DMPC within the monolayer is hardly reduced, and the DMPC surface concentration remains rather constant. Consequently, the ν(C═O) band intensity changes only slightly even when efficient hydrolysis occurs. Therefore, the lag time is estimated from the onset of the steady decrease of the monolayer area that starts with a high hydrolysis rate (Fig. 5).

3.3. PLA_2 activity probed by PM-IRRAS

Another approach to eliminate water vapor rotation–vibrations bands from IRRA spectra includes the polarization–modulation technique [33,34]. Thus, the trough shuttling procedure as used in IRRAS experiments is rendered unnecessary, and PM-IRRAS measurements can be accomplished in shorter time intervals. Hence, the temporal resolution is improved by a factor of ~2, and PM-IRRAS facilitates a more precise determination of the lag time of PLA_2 activity on the preferred conditions.

Fig. 6 shows sequences of PM-IRRA spectra collected from DMPC/chol (2:1, mol/mol) monolayers to test the PLA_2 lag phase at 12 and 13 mN/m. In these spectra, the ν(C═O) band is centered at 1736 cm^{-1} and oriented upward. This orientation of the absorption band occurs when the IR radiation incident at an angle of 75° probes a transition dipole moment preferentially aligned in the plane of the interface [33,34]. If the same transition dipole moment is sensed by *s*-polarized IR light, the corresponding band appears downward as seen for the C═O vibration in IRRAS spectra (cf. Fig. 3) [44].

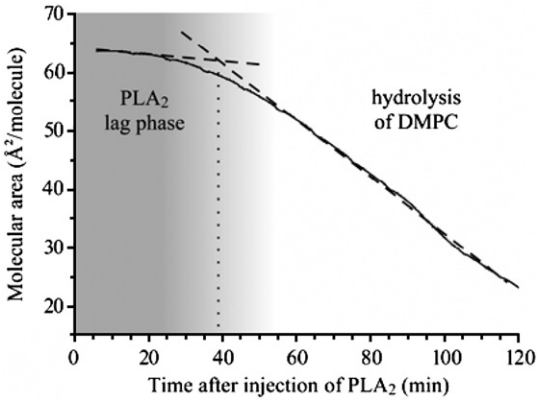

Fig. 5. Estimated lag time Δt of PLA_2 activity towards a pure DMPC monolayer at a constant surface pressure of 16 mN/m. The plot shows the molecular area of the film recorded as a function of time after the injection of 1 unit PLA_2 into the buffered subphase (solid line). The curve exhibits two linear regions corresponding to the PLA_2 lag phase (shaded in grey), where a slight area decrease is due to film instability, and to the hydrolysis of DMPC (white background), where the molecular area strongly declines because of the loss of reaction products from the monolayer. Two independent linear fits (dashed lines) are extrapolated to depict the intersection point. The respective time (dotted line) denotes the estimated lag time Δt of ~39 min.

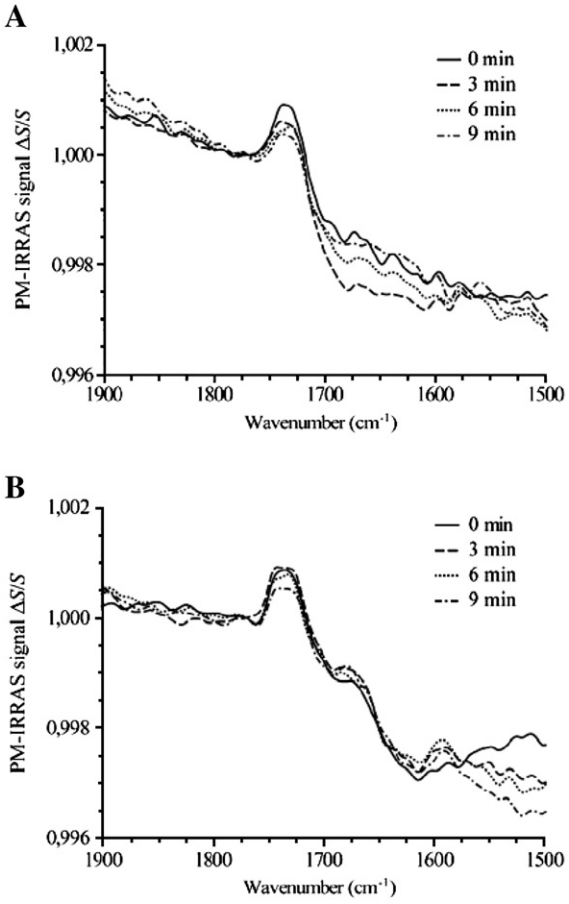

Fig. 6. PM-IRRA spectra of DMPC/chol (2:1, mol/mol) monolayers before and after injection of 1 unit PLA_2 into the buffered subphase. At surface pressures of 12 mN/m (A) and 13 mN/m (B), spectra were acquired before (solid line) and within 3; 6; and 9 min after PLA_2 injection (interrupted lines). All spectra are aligned at 1770 cm^{-1}.

At 12 mN/m, a continuous decrease of the ν(C═O) band intensity is observed from the very first measurement completed within 3 min after PLA_2 injection on (Fig. 6A). The pronounced reduction of the ν(C═O) absorption indicates that a substantial amount of DMPC is hydrolyzed within 3 min. We therefore conclude that the lag time of PLA_2 activity at 12 mN/m is not only shorter than our temporal resolution but also close to zero. This finding confirms our results obtained by IRRA spectroscopy. To further specify the surface pressure at which the PLA_2 lag phase first occurs, another set of experiments was performed at 13 mN/m (Fig. 6B). The first spectrum after enzyme injection depicts a similar intensity at 1736 cm^{-1} as the initial spectrum of the monolayer, but within 6 min, the beginning decrease of the ν(C═O) band and the onset of the hydrolytic activity of PLA_2 are perceived. Thus at 13 mN/m, the lag phase in PLA_2 activity Δt amounts to a minimum of 3 min.

Mean values of Δt as determined by PM-IRRAS are plotted in Fig. 7. The period before the onset of the enzymatic hydrolysis

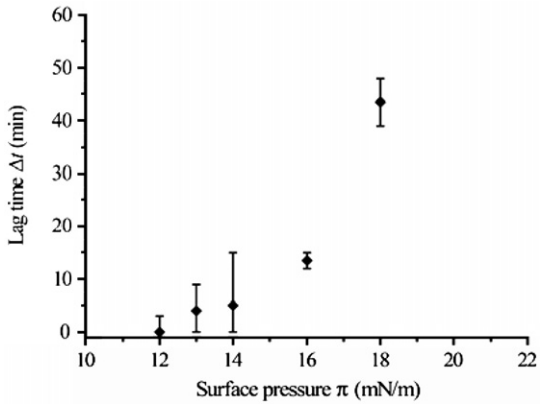

Fig. 7. Dependence of the lag time of PLA_2 activity Δt on the surface pressure π in mixed monolayers of DMPC/chol 2:1 (mol/mol) on a buffered subphase containing 1 unit PLA_2. Data points represent mean values of Δt from n PM-IRRAS experiments conducted at room temperature. $n=3$ for 12, 13, and 14 mN/m; $n=2$ for 16 and 18 mN/m.

of DMPC/chol (2:1, mol/mol) monolayers average to 1 min at 12 mN/m; 4 min at 13 mN/m; and 5 min at 14 mN/m. In general, the lag phases of 1 unit PLA_2 are slightly smaller when detected by PM-IRRAS instead of IRRAS. This difference is presumed to originate from the varying trough geometry of the two setups. During PM-IRRAS experiments, the PLA_2 concentration is somewhat reduced due to a greater subphase volume that possibly retards enzyme adsorption to the monolayer. However, this effect is apparently counter-balanced by a higher enzyme/lipid ratio and a mildly elevated temperature, which increases the PLA_2 activity. For these reasons, the duration of the PLA_2 lag phase slightly diverges for either experimental setup, but the correlation of the occurrence of the lag phase with the surface pressure of the DMPC/chol (2:1, mol/mol) monolayer is not influenced as the presented results show. In summary, the significant development of the lag time at $\pi \geq 12$ mN/m denotes a modification of the system at that surface pressure which crucially affects PLA_2 activity.

4. Discussion

Several investigations have suggested that the hydrolytic action of secretory PLA_2 ($sPLA_2$) on lipid membranes requires two consecutive steps: (1) localization of the enzyme at the membrane surface, and (2) the binding of a phospholipid molecule in the active site [43,45,46]. Whether PLA_2 adsorbs to or penetrates into the membrane before hydrolysis occurs is isoform-specific. Human PLA_2s from group IB and IIA have been found to significantly penetrate model membranes, whereas bee-venom PLA_2s (group III) do not [47,48]. It can be speculated that the cobra-venom PLA_2 (group IA) used in this study also employs a mechanism of substrate accession that is different from membrane penetration. This notion is supported by the absence of any amide bands in our (PM-) IRRA spectra during lipid hydrolysis. Similar observations have been made for DPPC monolayers [21]. There, snake-venom PLA_2 cannot be detected at surface pressures above 10 mN/m although hydrolysis proceeds. On the other hand, when this $sPLA_2$ is adsorbed to the pure air/buffer interface, amide bands are measurable. These data might suggest that snake-venom PLA_2 does not penetrate but adsorb to PC-containing monolayers. However, a direct evidence is missing. It is possible that the amount of $sPLA_2$ at the monolayer is simply too small to generate a signal that exceeds the bending vibration of liquid water located in the same wavenumber region as the amide bands. In fact, from neutron reflectivity studies, it is inferred that cobra-venom PLA_2 penetrates PC bilayers [49]. In summary, the localization of $sPLA_2$ is a complex issue that can range from slight adsorption to partial or deep penetration of the enzyme into the membrane. (This question could be solved through electron paramagnetic resonance spectroscopy of a site-selectively spin-labeled snake-venom PLA_2 in the presence or absence of membranes [47]).

The subsequent activation of $sPLA_2$ highly depends on the presence of heterogeneous, small-scale lateral structures within the lipid–membrane substrate like gel–fluid phase separation [10]. Exclusively fluid lipid bilayers can only be hydrolyzed if some kinds of membrane defect exist [50,51]. However, these concepts appear contradictory to the fact that cell membranes must feature full integrity and preferably fluidity to exert their biological functions. Hence, the question how $sPLA_2$s can be possibly activated under physiological conditions needs to be scrutinized. To this end, we examined if liquid–liquid immiscibility within a model membrane is sufficient to activate $sPLA_2$.

Using (PM-) IRRA spectroscopy, we have monitored the hydrolysis of DMPC/chol 2:1 (mol/mol) monolayers by $sPLA_2$ in time. Although the best temporal resolution was ~3 min, we have been able to identify the surface pressure that is critical to the occurrence of an enzymatic lag phase in this system. At 12 mN/m, the hydrolysis of the mixed monolayer starts right after $sPLA_2$ addition indicating an effective activation of the enzyme. At $\pi \geq 12$ mN/m, a lag phase of the hydrolytic activity is detected and increases exponentially with rising surface pressure. In this case, $sPLA_2$ activation is delayed. The corresponding lipid phase diagram allows us to correlate the surface pressure that is critical for enzyme activation with the lateral structure of the model membrane. For other lipid systems, it has already been shown that phase diagrams can be used to predict the activity of lipid-modifying enzymes [31,52]. Here, it turns out that $sPLA_2$ activity is indeed closely linked to the presence of coexisting liquid phases within the monolayer (cf. Fig. 1). At lower surface pressures, where different liquid domains are observed by epifluorescence microscopy, $sPLA_2$ is immediately active. At higher surface pressures, where the monolayer exhibits a homogenously fluid phase, enzyme activation is hampered. We assume that above the critical miscibility pressure (π_t), the macroscopically homogeneous monolayer still depicts some defects that eventually activate $sPLA_2$ according to the following rationale: the higher the surface pressure, the higher the lipid packing density, the less monolayer defects, the longer the lag phase. In addition, with increasing surface pressure, the C═O group of DMPC becomes less hydrated, i.e. less accessible to water molecules (unpublished results of B. Desbat), and might thus be less available to $sPLA_2$ attack in a similar way. However, this phenomenon is expected to be more important at higher surface pressures.

The critical miscibility pressure π_t itself depends on temperature and has been reported to be ~10 mN/m at 22 °C [53,54], ~11 mN/m at 24.5 °C [29], and ~12 mN/m at 25 °C [27]. The critical pressure for enzyme activation as determined in this study amounts to 12 mN/m at 20–22 °C and is slightly higher than expected from the phase diagram. This discrepancy can be explained by the varying lateral resolution of the applied techniques. Epifluorescence microscopy resolves domain structures on a micrometer scale and is furthermore highly dependent on the partitioning of the fluorescent probe [29]. Therefore, the existence of nano-heterogeneities cannot be precluded when homogeneous structures are observed near critical miscibility points. In contrast, the globular protein $sPLA_2$ displays a size of ~4 nm in diameter [55,56]. Thus, the enzyme can probe lateral structures in the nanometer range as it has been shown for lipid bilayers in the rippled phase state [24]. For this reason, in correspondence to the pressure range of $sPLA_2$ activation, the area of liquid–liquid immiscibility is further extended than described in the known phase diagram.

In summary, liquid–liquid phase heterogeneity is identified as another activating mechanism for $sPLA_2$s. With respect to physiological conditions, this concept combines two decisive membrane characteristics: fluidity and locally specific nanometer-scale structures. To be more precise, in monolayers of saturated PCs and cholesterol, condensed complexes are formed, which are correlated with the superlattice model and the liquid-ordered phase in lipid bilayers [57]. In fact, the initial activity of $sPLA_2$ is influenced by the extent of the cholesterol superlattice formed in mixed, liquid–crystalline phospholipid bilayers [58]. Furthermore, condensed complexes and liquid-ordered phases, respectively, are associated with the structure of membrane rafts [28,59]. Although the notion of rafts in biological membranes is still controversial, they are perceived as highly functional domains that incorporate a variety of membrane proteins [60]. Their domain boundaries may depict a preferred point of attack for $sPLA_2$s, which could thus generate lipid signaling molecules at the intersection of different signaling cascades.

Acknowledgements

The authors would like to thank Sarah L. Keller from the University of Washington for inspiring discussions. K.W. gratefully acknowledges receipt a short-term fellowship from the Federation of European Biochemical Societies (FEBS).

References

[1] F. Gambinossi, M. Puggelli, G. Gabrielli, Enzymatic hydrolysis reaction of phospholipids in monolayers, Colloids Surf., B Biointerfaces 23 (2002) 273–281.
[2] M. Murakami, I. Kudo, Phospholipase A(2), J. Biochem. 131 (2002) 285–292.
[3] J. Balsinde, M.V. Winstead, E.A. Dennis, Phospholipase A(2) regulation of arachidonic acid mobilization, FEBS Lett. 531 (2002) 2–6.
[4] S. Yedgar, Y. Cohen, D. Shoseyov, Control of phospholipase A(2) activities for the treatment of inflammatory conditions, BBA-Mol. Cell. Biol. Lipids 1761 (2006) 1373–1382.
[5] M. Nakanishi, D.W. Rosenberg, Roles of cPLA(2)alpha and arachidonic acid in cancer, BBA-Mol. Cell. Biol. Lipids 1761 (2006) 1335–1343.
[6] R.H. Schaloske, E.A. Dennis, The phospholipase A(2) superfamily and its group numbering system, BBA-Mol. Cell. Biol. Lipids 1761 (2006) 1246–1259.
[7] D.A. Six, E.A. Dennis, The expanding superfamily of phospholipase A(2) enzymes: classification and characterization, BBA-Mol. Cell. Biol. Lipids 1488 (2000) 1–19.
[8] W.J. Brown, K. Chambers, A. Doody, Phospholipase A(2) (PLA(2)) enzymes in membrane trafficking: mediators of membrane shape and function, Traffic 4 (2003) 214–221.
[9] W.R. Burack, R.L. Biltonen, Lipid bilayer heterogeneities and modulation of phospholipase A(2) activity, Chem. Phys. Lipids 73 (1994) 209–222.
[10] O.G. Mouritsen, T.L. Andersen, A. Halperin, P.L. Hansen, A.F. Jakobsen, U.B. Jensen, M.O. Jensen, K. Jorgensen, T. Kaasgaard, C. Leidy, A.C. Simonsen, G.H. Peters, M. Weiss, Activation of interfacial enzymes at membrane surfaces, J. Phys.-Condens. Mater. 18 (2006) S1293–S1304.
[11] J.A.F. Op den Kamp, M.T. Kauerz, L.L.M. Van Deenen, Action of pancreatic phospholipase A2 on phosphatidyl-choline bilayers in different physical states, Biochim. Biophys. Acta 406 (1975) 169–177.
[12] W.R. Burack, Q. Yuan, R.L. Biltonen, Role of lateral phase-separation in the modulation of phospholipase-A2 activity, Biochemistry 32 (1993) 583–589.
[13] T. Honger, K. Jorgensen, R.L. Biltonen, O.G. Mouritsen, Systematic relationship between phospholipase A(2) activity and dynamic lipid bilayer microheterogeneity, Biochemistry 35 (1996) 9003–9006.
[14] P. Hoyrup, K. Jorgensen, O.G. Mouritsen, Phospholipase A(2)—an enzyme that is sensitive to the physics of its substrate, Europhys. Lett. 57 (2002) 464–470.
[15] L.K. Nielsen, K. Balashev, T.H. Callisen, T. Bjornholm, Influence of product phase separation on phospholipase A(2) hydrolysis of supported phospholipid bilayers studied by force microscopy, Biophys. J. 83 (2002) 2617–2624.
[16] P. Hoyrup, O.G. Mouritsen, K. Jorgensen, Phospholipase A(2) activity towards vesicles of DPPC and DMPC-DSPC containing small amounts of SMPC, Biochim. Biophys. Acta, Biomembr. 1515 (2001) 133–143.
[17] D.W. Grainger, A. Reichert, H. Ringsdorf, C. Salesse, An enzyme caught in action — direct imaging of hydrolytic function and domain formation of phospholipase-A-2 in phosphatidylcholine monolayers, FEBS Lett. 252 (1989) 73–82.
[18] D.W. Grainger, A. Reichert, H. Ringsdorf, C. Salesse, Hydrolytic action of phospholipase-A2 in monolayers in the phase-transition region — direct observation of enzyme domain formation using fluorescence microscopy, Biochim. Biophys. Acta 1023 (1990) 365–379.
[19] A. Gericke, H. Hühnerfuss, IR reflection-absorption spectroscopy — a versatile tool for studying interfacial enzymatic processes, Chem. Phys. Lipids 74 (1994) 205–210.
[20] M. Grandbois, B. Desbat, C. Salesse, Monitoring of phospholipid monolayer hydrolysis by phospholipase A2 by use of polarization-modulated Fourier transform infrared spectroscopy, Biophys. Chem. 88 (2000) 127–135.
[21] U. Dahmen-Levison, G. Brezesinski, H. Möhwald, Enzymatic hydrolysis of monolayers: a polarization modulated-infrared reflection absorption spectroscopy study, Prog. Colloid Polym. Sci. 110 (1998) 269–274.
[22] M. Grandbois, H. Clausen-Schaumann, H. Gaub, Atomic force microscope imaging of phospholipid bilayer degradation by phospholipase A(2), Biophys. J. 74 (1998) 2398–2404.
[23] T. Kaasgaard, C. Leidy, J.H. Ipsen, O.G. Mouritsen, K. Jorgensen, In situ atomic force microscope imaging of supported lipid bilayers, Single Mol. 2 (2001) 105–108.
[24] C. Leidy, O.G. Mouritsen, K. Jorgensen, N.H. Peters, Evolution of a rippled membrane during phospholipase A(2) hydrolysis studied by time-resolved AFM, Biophys. J. 87 (2004) 408–418.
[25] P. Hoyrup, T.H. Callisen, M.O. Jensen, A. Halperin, O.G. Mouritsen, Lipid protrusions, membrane softness, and enzymatic activity, Phys. Chem. Chem. Phys. 6 (2004) 1608–1615.
[26] A. Halperin, O.G. Mouritsen, Role of lipid protrusions in the function of interfacial enzymes, Eur. Biophys. J. Biophys. Lett. 34 (2005) 967–971.
[27] S. Subramaniam, H.M. McConnell, Critical mixing in monolayer mixtures of phospholipid and cholesterol, J. Phys. Chem. 91 (1987) 1715–1718.

[28] H.M. McConnell, M. Vrljic, Liquid–liquid immiscibility in membranes, Annu. Rev. Biophys. Biomol. Struct. 32 (2003) 469–492.
[29] T.M. Okonogi, H.M. McConnell, Contrast inversion in the epifluorescence of cholesterol–phospholipid monolayers, Biophys. J. 86 (2004) 880–890.
[30] U. Dahmen-Levison, G. Brezesinski, Methyl-branched glycerophosphocholines: monolayer disorder and its effect on the rate of phospholipase A (2) catalyzed hydrolysis, Phys. Chem. Chem. Phys. 2 (2000) 4605–4608.
[31] C. Leidy, L. Linderoth, T.L. Andresen, O.G. Mouritsen, K. Jorgensen, G.H. Peters, Domain-induced activation of human phospholipase A2 type IIA: local versus global lipid composition, Biophys. J. 90 (2006) 3165–3175.
[32] C.R. Flach, J.W. Brauner, J.W. Taylor, R.C. Baldwin, R. Mendelsohn, External reflection FTIR of peptide monolayer films in-situ at the air/water interface — experimental-design, spectra-structure correlations, and effects of hydrogen–deuterium exchange, Biophys. J. 67 (1994) 402–410.
[33] D. Blaudez, T. Buffeteau, J.C. Cornut, B. Desbat, N. Escafre, M. Pezolet, J.M. Turlet, Polarization modulation FTIR spectroscopy at the air–water-interface, Thin Solid Films 242 (1994) 146–150.
[34] D. Blaudez, T. Buffeteau, J.C. Cornut, B. Desbat, N. Escafre, M. Pezolet, J.M. Turlet, Polarization-modulated FT-IR spectroscopy of a spread monolayer at the air–water-interface, Appl. Spectrosc. 47 (1993) 869–874.
[35] X.L. Wang, S.P. Zheng, Q. He, G. Brezesinski, H. Möhwald, J.B. Li, Hydrolysis reaction analysis of L-alpha-distearoylphosphatidylcholine monolayer catalyzed by phospholipase A(2) with polarization-modulated infrared reflection absorption spectroscopy, Langmuir 21 (2005) 1051–1054.
[36] M. Chaplin, Molecular Vibration and Absorption, in: M. Chaplin (Ed.), Water structure and behavior, Department of Applied Science, London South Bank University, 2007, http://www.lsbu.ac.uk/water/vibrat.
[37] A. Blume, W. Hübner, G. Messner, Fourier-transform infrared-spectroscopy of C-13=O-labeled phospholipids hydrogen-bonding to carbonyl groups, Biochemistry 27 (1988) 8239–8249.
[38] W. Hübner, H.H. Mantsch, Orientation of specifically C-13=O labeled phosphatidylcholine multilayers from polarized attenuated total reflection FT-IR spectroscopy, Biophys. J. 59 (1991) 1261–1272.
[39] V.V. Volkov, F. Nuti, Y. Takaoka, R. Chelli, A.M. Papini, R. Righini, Hydration and hydrogen bonding of carbonyls in dimyristoyl-phosphatidylcholine bilayer, J. Am. Chem. Soc. 128 (2006) 9466–9471.
[40] J.L.R. Arrondo, F.M. Goni, J.M. Macarulla, Infrared-spectroscopy of phosphatidylcholines in aqueous suspension—a study of the phosphate group vibrations, Biochim. Biophys. Acta 794 (1984) 165–168.
[41] W. Hübner, A. Blume, Interactions at the lipid–water interface, Chem. Phys. Lipids 96 (1998) 99–123.
[42] O. Albrecht, H. Matsuda, K. Eguchi, T. Nakagiri, The dissolution of myristic acid monolayers in water, Thin Solid Films 338 (1999) 252–264.
[43] H.P. Wacklin, F. Tiberg, G. Fragneto, R.K. Thomas, Distribution of reaction products in phospholipase A2 hydrolysis, Biochim. Biophys. Acta, Biomembr. 1768 (2007) 1036–1049.
[44] J.W. Brauner, C.R. Flach, Z. Xu, X.H. Bi, R. Lewis, R.N. McElhaney, A. Gericke, R. Mendelsohn, Quantitative functional group orientation in Langmuir films by infrared reflection-absorption spectroscopy: C═O groups in behenic acid methyl ester and sn2-C-13-DSPC, J. Phys. Chem., B 107 (2003) 7202–7211.
[45] L.B. Jensen, N.K. Burgess, D.D. Gonda, E. Spencer, H.A. Wilson-Ashworth, E. Driscoll, M.P. Vu, J.L. Fairbourn, A.M. Judd, J.D. Bell, Mechanisms governing the level of susceptibility of erythrocyte membranes to secretory phospholipase A(2), Biophys. J. 88 (2005) 2692–2705.
[46] M.K. Jain, O.G. Berg, Coupling of the i-face and the active site of phospholipase A(2) for interfacial activation, Curr. Opin. Chem. Biol. 10 (2006) 473–479.
[47] Y. Lin, R. Nielsen, D. Murray, W.L. Hubbell, C. Mailer, B.H. Robinson, M.H. Gelb, Docking phospholipase A(2) on membranes using electrostatic potential-modulated spin relaxation magnetic resonance, Science 279 (1998) 1925–1929.
[48] A.H. Pande, S. Qin, K.N. Nemec, X.M. He, S.A. Tatulian, Isoform-specific membrane insertion of secretory phospholipase A(2) and functional implications, Biochemistry 45 (2006) 12436–12447.
[49] H.P. Vacklin, F. Tiberg, G. Fragneto, R.K. Thomas, Phospholipase A(2) hydrolysis of supported phospholipid bilayers: A neutron reflectivity and ellipsometry study, Biochemistry 44 (2005) 2811–2821.
[50] U.B. Jensen, A.C. Simonsen, Shape relaxations in a fluid supported membrane during hydrolysis by phospholipase A(2), Biochim. Biophys. Acta, Biomembr. 1715 (2005) 1–5.
[51] A.C. Simonsen, U.B. Jensen, P.L. Hansen, Hydrolysis of fluid supported membrane islands by phospholipase A(2): Time-lapse imaging and kinetic analysis, J. Colloid Interface Sci. 301 (2006) 107–115.
[52] K. Wagner, G. Brezesinski, Phospholipase D activity is regulated by product segregation and the structure formation of phosphatidic acid within model membranes, Biophys. J. 93 (2007) 2373–2383.
[53] J.P. Slotte, Lateral domain heterogeneity in cholesterol phosphatidylcholine monolayers as a function of cholesterol concentration and phosphatidylcholine acyl-chain length, Biochim. Biophys. Acta, Biomembr. 1238 (1995) 118–126.
[54] J.P. Hagen, H.M. McConnell, Critical pressures in multicomponent lipid monolayers, Biochim. Biophys. Acta, Biomembr. 1280 (1996) 169–172.
[55] D.L. Scott, S.P. White, Z. Otwinowski, W. Yuan, M.H. Gelb, P.B. Sigler, Interfacial catalysis—the mechanism of phospholipase-A2, Science 250 (1990) 1541–1546.
[56] J.M. Winget, Y.H. Pan, B.J. Bahnson, The interfacial binding surface of phospholipase A2s, BBA-Mol. Cell. Biol. Lipids 1761 (2006) 1260–1269.
[57] S.L. Keller, A. Radhakrishnan, H.M. McConnell, Saturated phospholipids with high melting temperatures form complexes with cholesterol in monolayers, J. Phys. Chem., B 104 (2000) 7522–7527.
[58] F. Liu, P.L.G. Chong, Evidence for a regulatory role of cholesterol superlattices in the hydrolytic activity of secretory phospholipase A2 in lipid membranes, Biochemistry 38 (1999) 3867–3873.
[59] S.L. Veatch, S.L. Keller, Seeing spots: complex phase behavior in simple membranes, Biochim. Biophys. Acta, Mol. Cell Res. 1746 (2005) 172–185.
[60] K. Simons, D. Toomre, Lipid rafts and signal transduction, Nat. Rev., Mol. Cell Biol. 1 (2000) 31–39.